Journal of The Electrochemical Society, **147** (10) 3899-3906 (2000)
S0013-4651(00)02-007-3 CCC: $7.00 © The Electrochemical Society, Inc.

The Sensitivity of Thermal Donor Generation in Silicon to Self-interstitial Sinks

V. V. Voronkov,[a,*,z] G. I. Voronkova,[b] A. V. Batunina,[b] R. Falster,[c,*] V. N. Golovina,[b] A. S. Guliaeva,[b] N. B. Tiurina,[b] and M. G. Milvidski[b]

[a]*MEMC Electronic Materials, 39012 Merano BZ, Italy*
[b]*Institute of Rare Metals, 109017 Moscow, Russia*
[c]*MEMC Electronic Materials, 28100 Novara 1, Italy*

Thermal donor (TD) generation in silicon at 500°C was found to depend significantly on the cooling rate used after sequential annealing steps and on the nature of the ambient (air or vacuum). By performing the anneals initially under some specified cooling rate and ambient, and then changing to a new set of conditions, it was found that the TD concentration relaxed to the value corresponding to the new conditions. These results are well explained by a self-interstitial enhancement of TD generation rate. Self-interstitials are emitted by TD clusters, and their concentration, C_i, depends on the efficiency of sinks (sample surface, bulk voids). For vacuum annealing the major sink is the sample surface. For air anneals this sink is "passivated," presumably due to oxidation of the surface and/or by surface contamination, thus leaving only voids to act as self-interstitial sinks. Fast cooling seems to partly passivate voids (presumably by a decoration mechanism), further decreasing the sink efficiency, and therefore increasing C_i and the TD generation rate. The quantitative theory of sink-controlled TD generation provides a good description of the complicated experimental kinetic curves.

Manuscript submitted February 2, 2000; revised manuscript received July 5, 2000.

This work was initially intended to examine the effect of rapid thermal annealing (RTA) on the generation of thermal donors (TD) in silicon in the temperature range 450 to 500°C. RTA preanneals made at 1200°C in nitrogen were reported[1] to retard TD generation at 450°C for about 5 h, and so it was thought interesting to look at the temperature dependence of this retardation. Such an RTA-induced retardation was not found in the present study, however. The difference in the TD kinetics between as-grown and RTA samples was not significant, in accord with other recent data.[2] Instead of the expected retardation we observed another striking effect: it was noticed that the TD concentration was remarkably sensitive to the cooling rate of the sample after the TD-producing anneal steps. This effect was most evident for the RTA-treated samples annealed at 500°C, though it was found in as-grown samples too. The effect of annealing conditions on the TD kinetics is the subject of the present work.

Experimental

We used a set of wafers (0.675 mm thick) cut from the same crystal from adjacent positions and subjected to an RTA treatment at 1250°C for 35 s in nitrogen ambient. The crystal, 150 mm in diameter, was grown in the vacancy mode,[3] at the relatively high pull rate of 0.8 mm/min. The oxygen content was 1×10^{18} cm^{-3} (using the calibration factor 3.14×10^{17} cm^{-2}), and the carbon content was below the detection limit of 2×10^{15} cm^{-3}. The crystal was boron doped to the concentration $N_B = 1.7 \times 10^{15}$ cm^{-3}. Rectangular samples (12 mm long and 3 mm wide) were cut from the central part of the wafers.

The thermal donor generation anneals were performed in two different types of furnaces. One of these was an air ambient furnace and the other a vacuum furnace (the residual pressure was 10^{-3} Torr). The anneals were performed using sequential time steps of 4 h (in most cases). A total duration of up to 80 h was accumulated in this way. In the air furnace each of the sequential anneal steps was followed by one of two different cooling procedures: either quenching (placing a sample on a thick silicon plate) or slow cooling (leaving a sample inside the furnace after switching-off the power). The fast cooling rate was about 60 K/s, the slow cooling rate was about 0.2 K/s. The cooling curves, $T(t)$, were recorded using a thermocouple attached to a sample. After each of the annealing step the samples were slightly lapped so that the sample thickness was gradually reduced, finally down to 0.55 mm. In the vacuum tube furnace the cooling rate was fixed at about 0.8 K/s, intermediate between the slow and fast cooling conditions in the air furnace. The furnace temperature was controlled by a thermocouple, and maintained at prescribed value with the accuracy of 1°C for the vacuum furnace and 3°C for the air furnace.

The TD concentration was deduced from Hall effect measurements at temperatures down to liquid helium. An example of a temperature dependence of the electron concentration $n(T)$ in a TD containing sample is shown in Fig. 1. The electron concentration decreases upon lowering T due to the change in the charge state of the double TD, from doubly charged at room temperature to singly charged at liquid nitrogen temperature. Subsequent decrease in $n(T)$ upon the further lowering of T is caused by the capture of electrons by single-charged donors. The double TD family includes species of slightly different energy levels. The experimental curve is, however, well fitted by the theoretical temperature dependence of n on T (solid line) assuming that the double TD family is represented by one averaged deep level and one averaged shallow level. This fit provides both

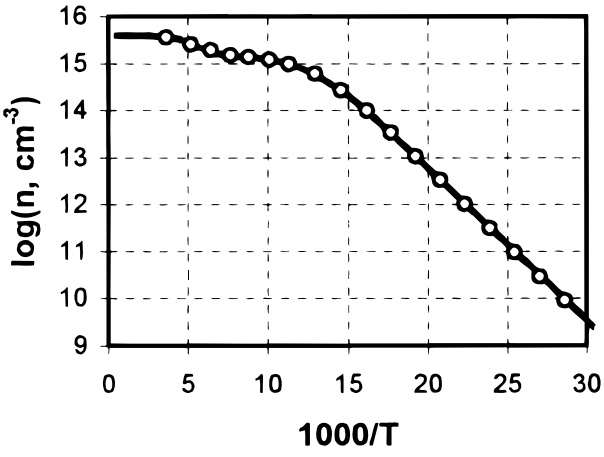

Figure 1. Representative data showing the temperature dependence of the electron concentration deduced from the Hall effect measured down to liquid helium temperature. The sample was annealed at 500°C in air (fast cooling mode) for 8 h. The deduced numbers: $N = 2.45 \times 10^{15}$ cm^{-3}, deep energy level is 133 meV, shallow energy level is 60 meV, $N_s = 7 \times 10^{14}$ cm^{-3} .

* Electrochemical Society Active Member.
z E-mail: vvoronkov@memc.com

S0013-4651(00)02-007-3 CCC: $7.00

the concentration of double donors, N [which is the difference between the two plateau values in $n(T)$], and the two averaged energy levels. The TD community generally includes also single-shallow donors, STD,[4,5] of concentration N_s. The room temperature electron concentration n_r equals $2N + N_s - N_B$, where N_B is the boron concentration. Once N is determined, the contribution of STD can be separated. It was found that N_s was always less than N. Therefore, N is nearly half of the added electron concentration at room temperature.

Results

Generation of TD at 500°C.—The dependence of the produced TD concentration, N, on the anneal time t at 500°C is shown in Fig. 2. The curve represented by circles corresponds to fast cooling after each anneal step performed in air. The curve represented by triangles corresponds to the slow cooling condition after each anneal step in air. The curve represented by squares is for the anneal performed in the vacuum furnace. The solid lines in this figure are computed according to the model discussed in the next section. The kinetic curve for the slow-cooling sequence is well below the one for fast-cooling sequence. The kinetic curve for annealing in the vacuum furnace is lower still.

A remarkable feature of $N(t)$ curves is that, after reaching saturation, N begins to decrease. Such a behavior had been reported earlier for prolonged anneals both at 500°C[6] and at lower T.[7-9]

The difference in the observed kinetic curves of Fig. 2 is not directly or simply correlated to the cooling rate. For example, the anneal in vacuum is of an intermediate cooling rate yet it produced the lowest TD concentration. The relevant factor responsible for the difference in $N(t)$ for the various annealing conditions is dependent on both the ambient and on the cooling rate. This (at the moment not specified) factor is abruptly changed if the anneal conditions are changed after some duration. This important effect is shown in Fig. 3. The two reference curves, labeled A and V, are for fixed anneal conditions: the anneals in air with fast cooling and the vacuum furnace anneals, respectively. These are reproduced from Fig. 2.

The curve A/V marked by filled squares in Fig. 3a corresponds to an initial 13 h anneal in air followed by further anneals in vacuum. Following the change in ambient, the TD concentration decays and approaches the lower values obtained for a vacuum-only anneal.

The curve V/A shown by filled circles in Fig. 3b corresponds to sequential anneals performed in the air furnace following an initial 19 h anneal in vacuum. In this case, the TD concentration increases after the change, and approaches the value characteristic for an air-only anneal, and even exceeds this value at longer duration.

Evolution of TD energy level.—The deep level of double TD, as deduced from the temperature dependence of electron concentration, is shown in Fig. 4 for the same three types of anneal conditions. Unlike the TD concentration, the (averaged) energy level is not very sensitive to the cooling rate or to the ambient, especially at shorter duration.

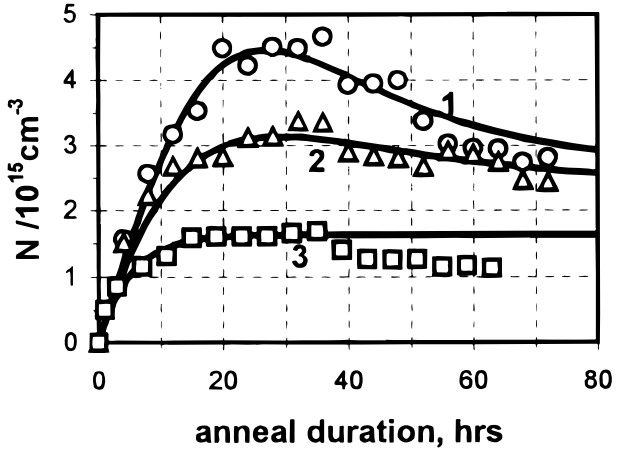

Figure 2. Kinetic curves at 500°C for RTA-pretreated samples. Curve 1 (circles) anneal in air with fast cooling; curve 2 (triangles) anneal in air with slow cooling; curve 3 (squares) anneal in vacuum. Solid lines are computed within the model of self-interstitial controlled agglomeration.

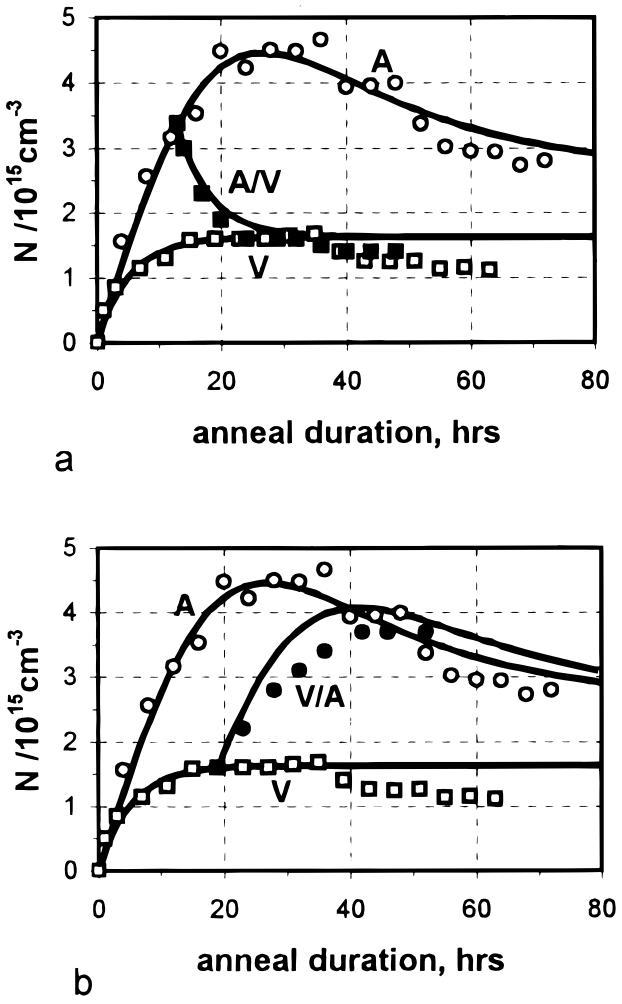

Figure 3. Effect of changing anneal conditions. (a) Anneal in vacuum, after initial anneal in air with fast cooling (curve A/V, filled squares); (b) anneal in air (with fast cooling), after initial anneal in vacuum (curve V/A, filled circles). The only-air and only-vacuum kinetic curves, A and V, respectively, are also shown for comparison. Solid lines are theoretical curves.

Generation of TD at 480 and 450°C.—A difference between the TD kinetic curves for annealing in air (with fast cooling) and for vacuum annealing is less pronounced at lower anneal temperature (Fig. 5). At 480°C the difference between the curves is still appreciable (Fig. 5a) while at 450°C anneal it is almost absent (Fig. 5b).

Evidence of microdefect (void) decoration by 480°C annealing.—The samples used in this study were grown in the vacancy mode and thus contained voids. Etching techniques were used to investigate these microdefects in both nonannealed samples and those annealed at 480°C, both in the air furnace (with fast cooling) and in the vacuum furnace. In nonannealed samples no etch patterns were revealed indicating that the grown-in voids are not revealed by this technique. On the other hand, a clear etch pattern was revealed (Fig. 6) following the anneals, especially the anneals in air. The surface pit density was converted into a bulk microdefect density by dividing it by the thickness of the etched-away layer. The deduced microdefect density is on the order of 10^6 cm^{-3} for air-annealed samples. This is a typical density for voids[10,11] in standard vacancy-type Czochralski (CZ) silicon crystals. We consider this result as evidence of void decoration by some contaminant during the anneal. In

S0013-4651(00)02-007-3 CCC: $7.00

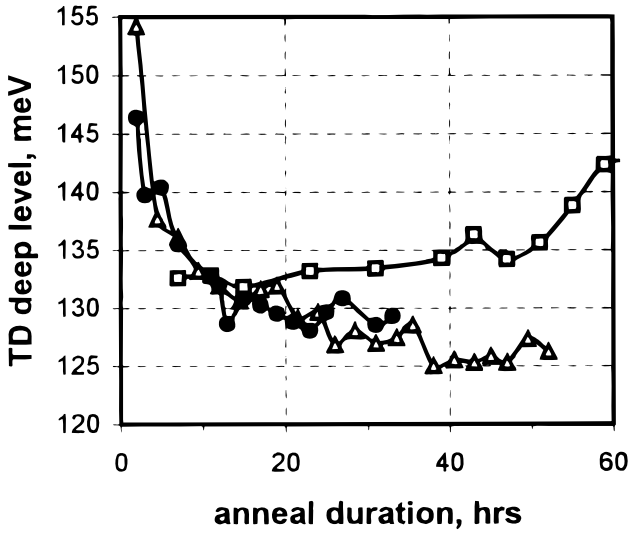

Figure 4. Deep energy level of double TD (filled circles: fast cooling in air; open triangles: slow cooling in air; open squares: vacuum furnace); anneal at 500°C.

general microdefects are much easier to reveal by etching if decorated by impurities.[12]

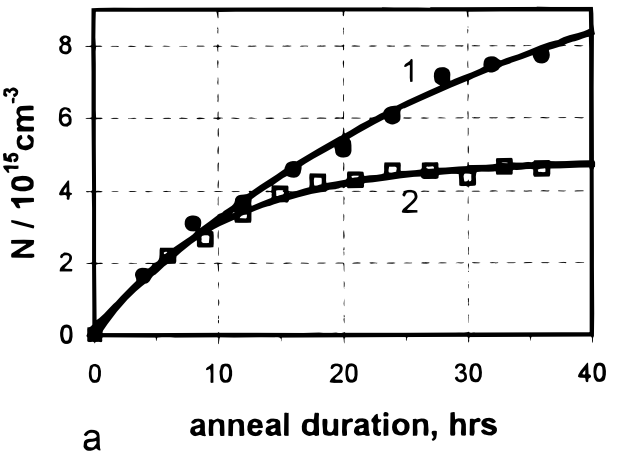

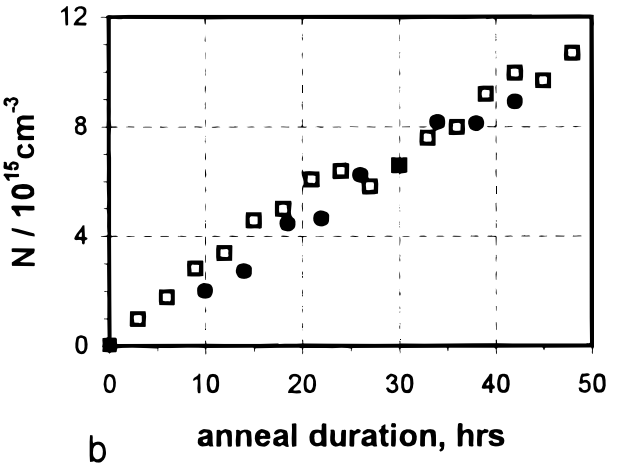

Figure 5. Comparison of annealing in air followed by fast cooling (filled circles) and anneal in vacuum (squares) at (a) 480 and (b) 450°C. Solid lines represent exponential fit, according to Eq. 12.

Model

The kinetics of TD formation is known to be affected by certain impurities such as carbon,[13,14] hydrogen,[15,16] or nitrogen.[17,18] Such an impurity effect is however considered to be irrelevant to the present discussion of the sensitivity of TD to the cooling rate and ambient. The studied samples, taken from adjacent wafers of the same crystal, are of the same impurity content. In particular, the impurity effect cannot account for the observed abrupt change in the shape of the kinetic curve caused by switching from initial anneal conditions to new ones (Fig. 3).

In order to account for the observations of sensitivity of the TD kinetics (at specified temperature and oxygen content) to the sample thermal history and annealing conditions we take into consideration the role of silicon self-interstitials. TD kinetics may be largely controlled by self-interstitials[19] emitted by oxygen clusters during the anneal. A self-interstitial (Si_i) may act, like hydrogen, as a catalyst for some reactions involved in TD production, accelerating those reactions and with them the TD generation rate.

The emitted Si_i species are consumed by sinks, sample surface, and bulk microdefects, and the self-interstitial concentration C_i resulting from this emission is thus strongly sensitive to the sinking efficiency. The sinking rate is generally proportional to the difference between C_i and the equilibrium self-interstitial concentration, but the latter is negligible[3] at temperatures as low as 500°C.

In vacancy-type silicon the bulk sinks are voids.[3] The interstitial flux to voids can be written in the form $\beta_v D_i C_i$ where D_i is the self-

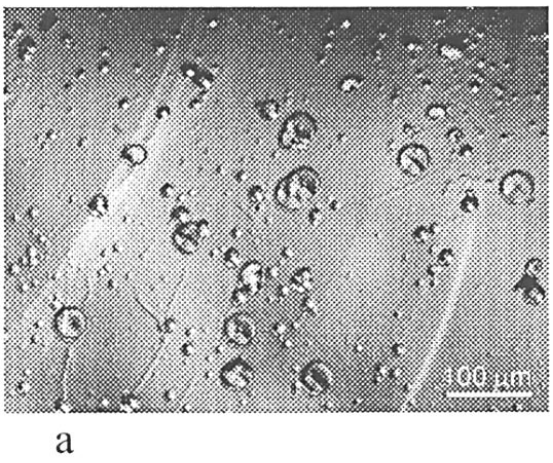

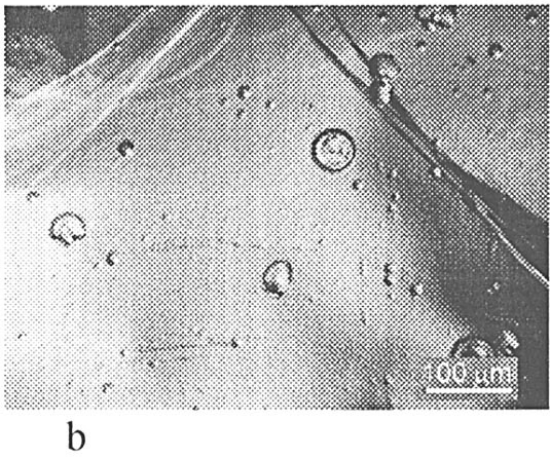

Figure 6. Etch pattern observed after anneal at 480°C, 24 h in (a) air furnace with fast cooling, (b) vacuum furnace. The scale mark is 100 μm. Samples were first polished in HF/HNO_3 solution and then etched in a Sirtl-like etchant.

S0013-4651(00)02-007-3 CCC: $7.00

interstitial diffusivity; the coefficient. β_v may be called the sinking efficiency of voids. For diffusion-limited flux, $\beta_v = 4\pi R_V N_V$ where R_V and N_V are the void radius and density. Typical numbers for R_V and N_V[3] correspond to $\beta_v = 150\ cm^{-2}$.

The loss rate of interstitials to the sample surface is similarly written as $\beta_s D_i C_i$ where C_i is now averaged over the depth, and the loss is normalized by the sample thickness d. For diffusion-limited sinking the depth profile $C_i(z)$ may be approximated by the first Fourier term, $\sin(\pi z/d)$. Within this approximation, the surface sinking efficiency $\beta_s = (\pi/d)^2 = 2000\ cm^{-2}$ (with $d = 675\ \mu m$). This is considerably higher than the void efficiency. The ratio of the two values, β_s/β_v, is about 14. When the two kinds of diffusion-limited sinks act simultaneously, the void contribution can be neglected.

The effect observed in the present paper, sensitivity of TD generation to the cooling rate and ambient, implies that the sink efficiency is actually strongly affected by the anneal conditions (and thus is not always diffusion limited).

The enhancement in TD concentration caused by changing the anneal ambient from vacuum to air can be easily understood if the major sink, the sample surface, is at full efficiency under the cleaner conditions of vacuum anneal [$\beta_s = (\pi/d)^2$] but completely passivated by air ambient ($\beta_s = 0$). This passivation may be due to an oxide film formed at the sample surface or/and surface contaminants. The loss of the major sink, the sample surface, by replacing the vacuum with air, will result in an increased self-interstitial concentration C_i. This effect is considered to be the main reason for a strong enhancement in TD generation (Fig. 2 and 3).

Further enhancement of TD generation in air ambients, by increasing the cooling rate, may be attributed to partial passivation of the remaining sinks, or voids, by fast diffusing contaminants. Such contaminants (like copper) penetrate into the sample from the outside of the sample during an anneal. In the course of slow cooling, the impurity out-diffuses to the sample surface leaving most of the voids unaffected; in this case β_v is close to $4\pi R_v N_v$. However, when the cooling rate is fast, the contaminants remain in the sample bulk to decorate a larger fraction of voids. When a sample is annealed again, the decorating impurity precipitates may partially dissolve, but the impurity will be recollected upon the next cooling. The repeated annealing steps would result in a stronger decoration of already decorated voids.

The decorated voids may completely lose their ability to consume self-interstitials, and then only the remaining nondecorated voids will act as sinks. This is equivalent to a reduction in the sink density below N_v. Another possibility is that the decorated voids still consume self-interstitials but at a rate lower than that limited by diffusion. In any case, void decoration is thought to considerably reduce their sinking efficiency β_v, which results in an increased C_i and, accordingly, enhanced TD generation.

Void passivation by contaminants is just a reasonable possibility supported by the observed anneal-induced void decoration (Fig. 6). Strictly speaking, we can only state that the sinking efficiency of a sample is somehow affected by the cooling rate. In the subsequent consideration, the sinking efficiency β is treated as a parameter that depends on the annealing conditions.

Generation rate of TD as a function of self-interstitial concentration.—The TD clusters are generated (nucleated) by sequential transitions within some chain of states. The two neighboring states of this chain, labeled by integers k and $k + 1$, differ either in the cluster size n (the number of clustered oxygen atoms) or in atomic arrangement. In the former case the transition is an attachment of the next oxygen atom. In the latter case the transition is a reconstruction. The steady-state nucleation rate G is defined by classical nucleation theory as a sum over the sequential transitions[20]

$$1/G = \Sigma\ 1/J_k \qquad [1]$$

where J_k is the flux from k to $k + 1$ for the particular case of equilibrium between the clusters and the solid solution of monomeric oxygen. The equilibrium cluster concentration, C_k, is defined by the law of mass action and is proportional to the nth power of the oxygen concentration. The flux J_k is a product of C_k and the transition frequency ν_k. Both kinds of transitions, oxygen attachment and reconstruction, can be enhanced by self-interstitials. The attachment frequency may be enhanced in the presence of fast-diffusing oxygen/interstitial complexes, OSi_I. The reconstruction can be enhanced (catalyzed) when a Si_I species arrives to become the nearest neighbor of an oxygen cluster. In both cases the transition frequency is a linear function of the self-interstitial concentration C_i. The equilibrium flux J_k is likewise a linear function of C_i

$$J_k = J_{ko} + \alpha_k C_i \qquad [2]$$

Here J_{ko} is the intrinsic flux, that in the absence of self-interstitials, and α_k is a catalytic coefficient for the Si_I-enhanced transition.

The sum in the right part of expression 1 is often controlled by only one, the smallest, flux J_k, and thus represents a bottleneck for nucleation. The corresponding state k is then a critical nucleus. For this particular case the nucleation rate G is reduced to J_k, and thus given by the linear expression

$$G = G_o + \alpha C_i \qquad [3]$$

The index of the critical nucleus is omitted.

It had been thought[19] that the emission of a self-interstitial by a cluster might also be one of the relevant transitions in the chain leading to TD clusters. In this view the initial cluster O_n is transformed, by emission, into a new cluster O_nV. This new cluster might also be created by adding a vacancy to the initial cluster O_n. That is, in fact, why it is denoted by O_nV. Vacancy-type clusters O_nV can be counted using a Pt-diffusion technique.[21,22] This technique was thought to measure the concentration of grown-in or quenched-in vacancies, but these vacancies are actually transformed into O_nV complexes at temperatures below 1020°C.[23] Therefore it is actually the O_nV species that are counted by the Pt diffusion. Similar to free vacancies, they too recombine with in-diffusing interstitial Pt atoms. The produced species are substitutional Pt atoms (countable by deep level transient spectroscopy) and O_n clusters which are dissolved fast at the Pt diffusion temperature (730°C).

The Pt diffusion technique was applied[24] to samples following the TD-producing 500°C anneal. It was found that such annealing treatments do indeed produce the O_nV species. The concentrations are low, however. Only about $10^{12}\ cm^{-3}$ were found after several hours. This number is much lower than the scale of TD concentration, $10^{15}\ cm^{-3}$, so that emission is a very slow process in comparison to TD production. Emission transitions, therefore, do not participate directly in TD generation. They are, however, very important as a factor determining the actual concentration of self-interstitials, C_i.

Balance equation for self-interstitial concentration.—We assume that the major emitters of self-interstitials are the TD clusters. Thus the total emission rate is μN, where μ is the emission frequency. This quantity can be roughly estimated to be on the order of $10^{-7}\ s^{-1}$ using the above-mentioned scale for the emission-produced concentration of O_nV clusters. In reality there is some distribution in size and emission ability of the TD clusters and μ thus represents an averaged value. The population of the TD species seems to rapidly achieve an average size of ten oxygen atoms per cluster, and this size then becomes independent of anneal time.[25] Thus μ can also be considered as roughly independent of anneal duration.

Emitted interstitials can be reabsorbed by the O_nV clusters of concentration N_v. The forward emission rate μN is balanced by the backward absorption rate, proportional to the $C_i N_v$ product, when the concentrations satisfy the mass-action law

$$C_i N_v / N = \chi \qquad [4]$$

where χ is the equilibrium reaction constant (again averaged over the TD species).

The interstitial concentration is changed by all of the above-mentioned processes (emission, absorption by O_nV, and sinking)

$$dC_i/dt = \mu(N - N_v C_i/\chi) - \beta\eta D_i C_i \qquad [5]$$

S0013-4651(00)02-007-3 CCC: $7.00

The sinking efficiency β is strongly sensitive to the anneal conditions. For annealing in air, β is reduced to β_v. For annealing in vacuum, when the interstitial diffusion to the sample surface is important, the actual equation for the self-interstitial depth profile $C_i(z, t)$ will differ from Eq. 5 by including the diffusion term $D_i\partial^2 C_i/\partial z^2$ and retaining the bulk sinking to voids, $\beta_v D_i C_i$. However, on approximating the profile by the first Fourier term, $\sin(\pi z/d)$, one reduces the precise equation to an approximate Eq. 5, with $\beta = \beta_s + \beta_v$. Actually β is close to β_s in this case.

Diffusion of Si_I seems to be very fast even below the room temperature[26] implying a very low migration energy. The melting point value of D_i is high, about 3×10^{-4} cm^2/s,[27] also implying a low migration energy. When extrapolated down to 500°C, with a tentative migration energy of 0.25 eV, D_i is about 4×10^{-5} cm^2/s. The time scale of the self-interstitial relaxation to the steady-state value is shorter than $1/\beta D_i$ according to Eq. 5 and therefore less than 3 min, even if only voids act as sinks. Though the value of D_i at 500°C is not quite certain, the relaxation time $1/\beta D_i$ is assumed to be essentially shorter than the duration of an anneal step, 4 h. The current value of C_i is then almost steady-state, it corresponds to the zero right part of Eq. 5

$$C_i = \mu N/(\beta D_i + \mu N_v/\chi) \quad [6]$$

Initially, when the O_nV clusters are of low concentration, the first term in the denominator of this expression dominates, and C_i increases in proportion to the thermal donor concentration N

$$C_i = \mu N/\beta D_i \quad [7]$$

The TD production becomes progressively enhanced if β is not high. At a later stage of the anneal N becomes limited while N_v continues to increase as a result of emission and subsequent sinking of self-interstitials. The term $\mu N_v/\chi$ in the denominator of Eq. 6 then becomes dominant and C_i will decrease, resulting in a reduced generation rate G. This effect is the main reason for the decreasing portions of the kinetic curves 1 and 2 in Fig. 2.

Kinetic equation for TD concentration.—TD clusters are produced at the rate G specified by Eq. 3. Previously produced TD can be lost as is seen in the decreasing portions of kinetic curves in Fig. 2 and 3. The TD loss is characterized by some lifetime τ. The TD concentration evolves due to both generation and loss

$$dN/dt = G_o + \alpha C_i - N/\tau \quad [8]$$

There may be two qualitatively different loss mechanisms: (*i*) backward dissociation of TD clusters and (*ii*) transformation of TD clusters into some electrically inactive atomic configuration denoted by O_n^*, either by reconstruction or by reaching some threshold size at which the electrical activity is lost.

By the first mechanism the TD concentration N would reach the equilibrium value that depends only on the oxygen content C and is proportional to C^n (where n is the cluster size). The difference in the TD saturation level at medium duration (Fig. 2) cannot be explained by this alone.

The TD loss is therefore assumed to result from the transformation of O_n (TD clusters) into neutral O_n^* species. These species may also emit Si_I, but we do not include them in the basic balance Eq. 6 assuming that they are of much lower emission frequency than the TD clusters.

The lifetime τ is assumed independent of C_i , though in principle τ, like G, could be affected by self-interstitials. The assumption is justified by a good agreement of the computed kinetic curves with the experimental ones. Another argument in favor of τ being independent of C_i is the observed evolution of the energy level of TDs (Fig. 4). The deduced TD level is averaged over the prevailing TD species of various sizes. Smaller size means a deeper level.[28] A difference in the lifetime would induce a difference in the average size of the TDs: at shorter τ the clusters would reach a smaller size, and the observed energy level would be deeper. Since the level evolution is almost independent of the cooling rate for anneal in air, the TD lifetime also appears identical. The level evolution found for anneal in vacuum (squares in Fig. 4) is similar to that found in air, with only a slight difference at longer duration.

The kinetic Eq. 8, together with expression 6 for C_i, is already enough to understand qualitatively the abrupt changes in the shape of kinetic curves (Fig. 3) caused by switching the anneal conditions. This is caused by an abrupt change in the sink efficiency β.

When the anneal ambient is changed from air (low $\beta = \beta_v$) to vacuum (high $\beta \approx \beta_s$), the concentration C_i, as defined by Eq. 6, is abruptly decreased, and the right part of Eq. 8 is decreased accordingly, from an initial positive value to a negative value. A rising branch of $N(t)$ is immediately replaced by a decreasing branch (Fig. 3a).

When the conditions are changed from vacuum to air, β is sharply decreased, leading to an abruptly increased C_i. The derivative dN/dt then jumps from an initially low value to a large one (Fig. 3b).

Kinetic equation for O_nV clusters.—The kinetic Eq. 8 is not sufficient for describing the kinetic curve $N(t)$, since it includes the self-interstitial concentration C_i which is dependent on the accumulated concentration of O_nV clusters, N_v.

The concentration N_v is changed both by emission of self-interstitials by TD clusters and by backward absorption

$$dN_v/dt = \mu(N - C_i N_v/\chi) \quad [9]$$

With the steady-state value of C_i, as given by Eq. 6, the accumulation rate dN_v/dt becomes identical to the interstitial flux to sinks, βC_i.

Analytical solution for the initial stage of anneals.—With the simplified expression 7, applicable at an early stage of the anneal, the TD kinetic Eq. 8 is reduced to the conventional form of exponential relaxation

$$dN/dt = G_o - N/\tau_a \quad [10]$$

The effect of Si_I is reduced to replacing the genuine lifetime τ with the apparent sink-dependent lifetime τ_a

$$1/\tau_a = 1/\tau - \mu\alpha/\beta D_i \quad [11]$$

The apparent lifetime is always larger than τ. It is near the value τ only for high sink efficiency. The TD concentration increases exponentially up to the saturation value of $G_o\tau_a$

$$N = G_o\tau_a[1 - \exp(-t/\tau_a)] \quad [12]$$

The first half of the kinetic curves in Fig. 2 can be qualitatively described by this simplified theory of TD production. In particular for anneal in vacuum, the numerical results (described below) demonstrate that the concentration C_i is too low to enhance TD production. This is due to a relatively large β. In this case the apparent lifetime is identical to τ.

Numerical results.—The two kinetic Eq. 8 and 9, together with expression 6 specifying C_i as a function of N and N_v, provide a complete description of the cluster production including the TD component. For the purpose of numerical solution, it is convenient to scale the relevant variables N, N_v, and C_i: the scale for the TD concentration is $S = G_o\tau$; the scale for the O_nV concentration is $S_v = \alpha\chi\tau$; the scale for the self-interstitial concentration is $S_i = G_o/\alpha$.

The three scaled (divided by the scaling constants) variables are denoted by small letters n, n_v, and c_i, respectively. The equations for the scaled variables take a simple form

$$dn/dx = 1 + c_i - n \quad [13]$$

$$dn_v/dx = (n - c_i n_v)/A \quad [14]$$

$$c_i = n/(n_v + B) \quad [15]$$

where $x = t/\tau$ is the scaled time. The problem contains two dimensionless parameters, A and B. Parameter A is a normalized catalytic coefficient

$$A = \alpha\chi/G_o\mu\tau \quad [16]$$

S0013-4651(00)02-007-3 CCC: $7.00

while B is a normalized sink efficiency

$$B = \beta D_i/\alpha\mu\tau \quad [17]$$

The TD scale, $S = G_o\tau$, is identical to the saturated concentration for the vacuum anneal. It equals 1.6×10^{15} cm^{-3} (neglecting a reduction in N at a prolonged anneal which is not described by the present model). The lifetime τ was fitted to be 5 h; accordingly the intrinsic generation rate G_o equals 8.6×10^{10} cm^{-3} s^{-1}.

The catalytic parameter A was scanned over a wide range, and the two sink parameters B (for the two cases of annealing in air) were fitted at every A to get the best possible description of the two experimental curves (1 and 2 in Fig. 2). The parameter B for annealing in vacuum is not an independent one, *i.e.*, it is larger than that for air anneal with slow cooling by a factor of 14, as discussed above.

A good fit can be obtained within quite a wide range of A, but the best fit is for A close to 20. The fitted sink parameters, B, are only slightly dependent on the assumed value of A. The best fit numbers are for air anneal with fast cooling $B = 1.1$; for air anneal with slow cooling $B = 1.6$; for vacuum anneal $B = 22$.

The curve shape is very sensitive to the value of B for the case of air anneal, and the accuracy of B is better than 10%. The large value of B for vacuum annealing implies, according to Eq. 13 and 15, that the self-interstitial effect on TD generation is negligible for these anneal conditions.

The computed curves for the above set of parameters are plotted in Fig. 2 (solid lines).

The switching of anneal conditions at some point in the anneal sequence (Fig. 3) was simulated by an appropriate change in B at this point, from 1.1 to 22 in the case of Fig. 3a, and from 22 to 1.1 in the case of Fig. 3b. The transient portions of the kinetic curves are computed without the application of any additional fitting. Although the computed transient curves (Fig. 3) deviate somewhat from the measured ones, there is a good qualitative agreement between them.

Simulation of the TD kinetics provides not only the TD concentration $N(t)$ but also the time dependence of the other two relevant variables, $N_v(t)$ and $C_i(t)$. The scaled curves for all the three variables are shown in Fig. 7, using the three values of B listed above. The scaling parameters for the time and the three concentrations are summarized in Table I (the scales S_i and S_v are estimated in the next section). The self-interstitial concentration (Fig. 7b) first increases and then decreases, as already qualitatively explained. The kinetic curves for TD concentration (Fig. 7a) roughly follow this variation in $C_i(t)$. The concentration of the vacancy-type clusters N_v is gradually accumulated (Fig. 7c).

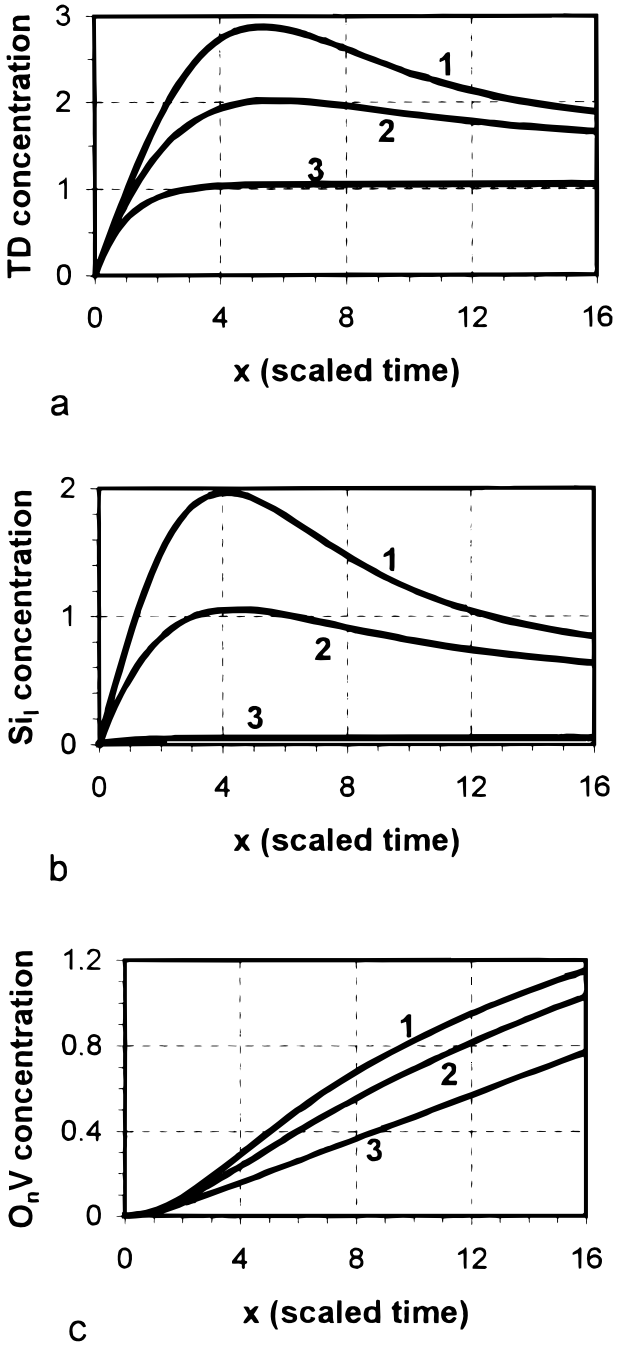

Figure 7. Computed (scaled) concentrations of (a) thermal donors, (b) self-interstitials, (c) vacancy-type complexes O_nV, for three representative values of sink parameter B (curves 1, 2, 3 correspond to $B = 1.1$, 1.6, and 22, respectively).

Discussion

Estimation of the model parameters.—The fitting procedure defines only two specific combinations (A and B) of the model parameters. Since the emission frequency μ was estimated above to be 10^{-7} s^{-1}, some other parameters can now be estimated, too. The product $\alpha\chi$ is about 3×10^9 cm^{-3} s^{-1}, according to Eq. 16. The parameter α/D_i is then deduced from Eq. 17, since the sink efficiency is known for the case of nonpassivated void sinks ($\beta = \beta_v = 150$ cm^{-2}) corresponding to the air anneal with slow cooling ($B = 1.6$). The resulting estimate is $\alpha/D_i = 5 \times 10^4$ cm^{-2}. With $\alpha\chi$ already estimated, the $D_i\chi$ product is found to be 6×10^4 cm^{-1} s^{-1}. With $D_i = 4 \times 10^{-5}$ cm^2/s, the catalytic coefficient α is 2 s^{-1}, and the emission equilibrium constant χ is 1.5×10^9 cm^{-3}.

Next, the concentration scales S_v and S_i can be specified, to convert the dimensionless plots of Fig. 7b and c into actual numbers. The scale S_v for the O_nV cluster concentration is $\alpha\chi\tau$, and it equals 6×10^{13} cm^{-3}, and the scale for the D_iC_i product is D_iG_o/α; it equals 1.6×10^6 cm^{-1} s^{-1}. The self-interstitial concentration scale is then $S_i = 4 \times 10^{10}$ cm^{-3}.

The most important consequence of the above estimates is that the O_nV clusters are poor absorbers of Si_I. Indeed, the absorption rate (which can be also called the recombination rate of O_nV and Si_I species) is RC_iN_v where the recombination coefficient R is identical to μ/χ, according to Eq. 9. If the recombination were diffusion limited, the coefficient R would be $4\pi rD_i$, where r is the reaction radius (on the order of the atomic distance, 3×10^{-8} cm). The ratio of the

Table I. Scaling parameters for the simulated kinetic curves of Fig. 7.

Time scale τ (h)	Thermal donor scale, S (cm^{-3})	Thermal donor scale, S_i (cm^{-3})	OnV cluster scale, S_v (cm^{-3})
5	1.6×10^{15}	4×10^{10}	6×10^{13}

S0013-4651(00)02-007-3 CCC: $7.00

Table II. Estimated parameters of TD generation model (at 500°C).

Emission frequency, μ (s^{-1})	Catalytic coefficient, α (s^{-1})	Emission constant, χ (cm^{-3})	Recombination coefficient, R (cm^3/s)
10^{-7}	2	1.5×10^9	7×10^{-17}

actual and diffusion-limited values of R is thus $\mu/(4\pi r D_i \chi) = 4 \times 10^{-6}$. This very low number implies that there is a considerable barrier E_r for recombination of Si_I with O_nV, reducing the reaction rate by a factor of $\exp(-E_r/kT)$. The estimated reduction corresponds to $E_r = 0.82$ eV.

The estimated parameters of the model (at 500°C) are summarized in Table II.

We are also able to estimate the activation energy for the lifetime τ using a simple conventional formula for the reconstruction reaction frequency $1/\tau$

$$1/\tau = \nu \exp(-E/kT) \quad [18]$$

The frequency prefactor ν is on the order of 10^{13} s^{-1}, and E is the energy barrier. The value of $\tau = 5$ h at 500°C corresponds to $E = 2.65$ eV.

In a similar way, the activation energy for emission frequency μ is estimated to be 3.1 eV. The recombination barrier (0.82 eV) specifies the activation energy for the combination $\mu/D_i\chi$. The activation energy for the $D_i\chi$ product is then 2.3 eV. The emission constant χ is characterized by the activation energy of 2 eV (with the assumed low migration energy for Si_I).

Criterion for simplified exponential TD kinetics.—It was noted above that at the first stage of the anneal the self-interstitial concentration is defined by a simplified Eq. 7 which is equivalent to $c_i = n/B$. The concentration of O_nV clusters, estimated from Eq. 14, is on the order of x/A if x is on the order of 1 or larger. The criterion for neglecting interstitial absorption by O_nV species, $n_v << B$, is fulfilled if x is smaller than AB (which is on the order of 20 or larger). The simplified Eq. 12 is applicable if the duration t does not exceed the lifetime τ by too much.

The shape of N(t) kinetic curve at lower T.—One of the important effects of reduced T is a remarkable increase in the lifetime τ. With an activation energy E now specified, one can obtain τ for other temperatures: $\tau = 15$ h at 480°C, and $\tau = 80$ h at 450°C. The scaled time $x = t/\tau$ is therefore considerably smaller at lower T in comparison to that at 500°C. In the range of small x, the TD kinetic curves are less sensitive to the sinking efficiency than at larger x (Fig. 7a). This is the main reason for the reduced difference between the experimental curves at lower T.

Since the kinetic curves at lower T correspond to a range of moderate scaled time $x = t/\tau$, they are described by Eq. 12, and the apparent lifetime τ_a can be deduced. For air annealing at 480°C (Fig. 6a, curve 1) the apparent lifetime τ_a is 34 h. This is certainly larger than τ. The ratio τ/τ_a is about 0.37. Equation 11 is equivalent to $\tau/\tau_a = 1 - 1/B$, and parameter B is estimated to be about 1.7. This value for B is not much different from that found at 500°C, $B = 1.1$.

Fraction of decorated voids.—The difference in the sink efficiency B between fast and slow cooling in air is not very large. They differ by only a factor of 1.5. If the void passivation mechanism is accepted to account for the difference, then the fraction of voids passivated by fast cooling is only one-third. Generally, decoration of microdefects by copper and nickel were indeed found to be only partial and cooling rate dependent, respectively.[12]

Effect of sample thickness on TD generation.—An important prediction of this model (not checked in the present study) is that TD generation in vacuum ambient should be remarkably enhanced by increasing the sample thickness d (and thus reducing the sink efficiency in proportion to $1/d^2$). This effect would saturate at a thickness larger than about 3 mm, when the efficiency of the surface sink becomes less than that of voids. The TD concentration would strongly decrease from the sample center to the surface following the depth profile of C_i. A depth-dependent enhancement of TD generation in thicker samples was indeed reported,[29] but under the conditions of that work the relevant catalyst might be hydrogen rather than Si_I.

Effect of oxygen loss.—The formation of oxygen clusters, both O_n (TD) and O_n^* (neutral species), results in a gradually reduced concentration of monomeric oxygen. Then the parameters of the generation rate, both G_o and α, gradually decrease with anneal time t. This effect was neglected above, for the sake of clarity of the model. However, it may change the shape of the kinetic curves, especially at longer anneal. The refined theory of TD production, taking into account the oxygen loss, is rather complicated, and it will be analyzed elsewhere.

Conclusions

Identical silicon samples were sequentially annealed under different conditions: in air or in vacuum, under fast cooling or under slow cooling after each anneal step. A systematic and significant sensitivity of the TD kinetic curve to the anneal conditions was found. The difference in the absolute value of the TD concentration may amount to a factor of three if the vacuum anneal is compared to that in air (with fast cooling).

These results are considered as a definite indication to the crucial role of self-interstitials (Si_I) in the production of thermal donors. The TD generation rate is essentially enhanced at higher Si_I concentration, C_i. The value of C_i is in turn controlled by the available sinks for Si_I. In vacuum annealing conditions the major sink is the sample surface. Under these conditions the concentration C_i is too low to affect TD generation. If however, the surface is passivated by annealing in air, the bulk sinks (voids in the present case) play the main role. These bulk sinks can be also partly (but not strongly) passivated if the cooling rate after the TD-producing anneal steps is fast. This effect is attributed to partial decoration of voids by a surface contaminant which in-diffuses during the anneal, remaining in the bulk under fast cooling conditions.

The quantitative theory of Si_I-enhanced TD production includes two kinetic equations, one for TD clusters and the other for the vacancy-type clusters, O_nV. These species are produced from thermal donors by emission. They are important as Si_I absorbers at longer anneal duration. For shorter anneals the sink effect on TD generation is much simplified and reduces to the replacing of the actual TD lifetime by some apparent lifetime which increases on decreasing the sink efficiency.

Though the experimental kinetic curves are of considerable scatter (which is understandable taking into account a random variation in the sink efficiency), they are well described, on average, by the proposed theory of Si_I-controlled oxygen agglomeration.

MEMC Electronic Materials assisted in meeting the publication costs of this article.

References

1. C. Maddalon-Vinante, J. P. Vallard, and D. Barbier, *J. Electrochem. Soc.*, **142,** 560 (1995).
2. H. Takeno, K. Aihara, Y. Hayamizu, T. Masai, and M. Suezawa, in *Defects in Silicon III*, T. Abe, W. M. Bullis, S. Kobayashi, W. Lin, and P. Wagner, Editors, PV 99-1, p.150, The Electrochemical Society Proceedings Series, Pennington NJ (1999).
3. V. V. Voronkov and R. Falster, *J. Cryst. Growth*, **194,** 76 (1998).
4. J. A. Griffin, J. Hartung, J. Weber, N. Navarro, and L. Genzel, *Appl. Phys. A*, **48,** 47 (1989).
5. A. Hara, M. Aoki, M. Koizuka, and T. Fukuda, *J. Appl. Phys.*, **75,** 2929 (1994).
6. V. M. Babich, N. P. Baran, Yu. P. Dotsenko, K. I. Zotov, V. B. Kovalchuk, and V. B. Maksimenko, *Phys. Techn. Semicond.*, **26,** 447 (1992) in Russian.
7. W. Kaiser, H. L. Frisch, and H. Reiss, *Phys.Rev.*, **112,** 1546 (1958).
8. T. Y. Tan, R. Kleinhenz, and C. P. Schneider, in *Oxygen, Carbon, Hydrogen, and Nitrogen in Crystalline Silicon*, J. C. Mikkelsen, S. J. Pearton, J. W. Corbett, and S. J. Pennycook, Editors, PV 59, p. 195, The MRS Proceedings Series, Pittsburgh, PA (1986).

S0013-4651(00)02-007-3 CCC: $7.00

9. Y. Kamiura, F. Hashimoto, and M. Yoneta, *J. Appl. Phys.*, **65,** 600 (1989).
10. K. Takano, M. Iida, E. Iino, M. Kimura, and H. Yamagishi, *J. Cryst. Growth*, **180,** 363 (1997).
11. T. Saishoji, K. Nakamura, H. Nakajima, T. Yokoyama, F. Ishikawa, and J. Tomioka, in *High Purity Silicon, V,* C. L. Claeys, P. Rai-Choudhury, M. Watanabe, P. Stallhofer, and H. J. Dawson, Editors, PV 98-13, p. 170, The Electrochemical Society Proceedings Series, Pennington, NJ (1998).
12. R. Falster, Z. Laczik, G. R. Booker, A. R. Bhatti, and P. Torok, in *Defect Engineering in Semiconductor Growth, Processing and Device Technology,* S. Ashok, J. Chevallier, K. Sumino, and E. Weber, Editors, PV 262, p. 945, MRS Proceeding Series, Pittsburgh, PA (1992).
13. A. R. Bean and R. C. Newman, *J. Phys. Chem. Solids,* **33,** 255 (1972).
14. J. Leroueille, *Phys. Status Solidi A,* **67,** 177 (1981).
15. R. C. Newman, A. R. Brown, R. Murray, A. Tipping, and J. H. Tucker, in *Semiconductor Silicon 1990,* H. R. Huff, K. G. Barraclough, and J. Chikawa, Editors, PV 90-7, p. 734, The Electrochemical Society Proceedings Series, Pennington NJ (1990).
16. H. J. Stein and S. Hahn, in *Defect Control in Semiconductors,* K. Sumino, Editor, p. 211, Elsevier, Amsterdam (1990).
17. C. S. Chen, C. F. Li, H. J. Ye, S. C. Shen, and D. R. Yang, *J. Appl. Phys.*, **76,** 3347 (1994).
18. D. Yang, R. Fan, L. Li, D. Que, and K. Sumino, *J. Appl. Phys.*, **80,** 1493 (1996).
19. V. V. Voronkov, *Semicond. Sci. Technol.*, **8,** 2037 (1993).
20. R. P. Andres, M. Boudart, *J. Chem. Phys. Solids*, **42,** 2055 (1965).
21. M. Jacob, P. Pichler, H. Ryssel, and R. Falster, *J. Appl. Phys.*, **82,** 182 (1997).
22. M. Jacob, P. Pichler, H. Ryssel, R. Falster, M. Cornara, D. Gambaro, M. Olmo, and M. Pagani, *Solid State Phenom.*, **57/58,** 349 (1997).
23. V. V. Voronkov and R. Falster, *J. Cryst. Growth*, **204,** 462 (1999).
24. M. Jacob, P. Pichler, and R. Falster, Unpublished results.
25. S. A. McQuaid, M. J. Binns, C. A. Londos, J. H. Tucker, A. R. Brown, and R. C. Newman, *J. Appl. Phys.*, **77,** 1427 (1995).
26. G. D. Watkins, in *Defects in Silicon III,* T. Abe, W. M. Bullis, S. Kobayashi, W. Lin, and P. Wagner, Editors, PV 99-1, p. 38, The Electrochemical Society Proceedings Series, Pennington, NJ (1999).
27. V. V. Voronkov and R. Falster, *J. Appl. Phys.*, **86,** 5975 (1999).
28. P. Wagner and J. Hage, *Appl. Phys. A,* **49,** 123 (1989).
29. A. Hara, M. Koizuka, M. Aoki, T. Fukuda, H. Yamada-Kaneta, and H. Mori, *Jpn. J. Appl. Phys.*, **33,** 5577 (1994).